Effects of Poly(methyl methacrylate)-Based Low-Profile Additives on the Properties of Cured Unsaturated Polyester Resins. II. Volume Shrinkage Characteristics and Internal Pigmentability

Jyh-Ping Dong, Jyh-Gau Huang, Fuh-Huah Lee, Jiunn-Wei Roan, Yan-Jyi Huang

Department of Chemical Engineering, National Taiwan University of Science and Technology, Taipei, Taiwan 106, Republic of China

Received 18 October 2002; accepted 25 August 2003

ABSTRACT: The effects of three series of self-synthesized poly(methyl methacrylate) (PMMA)-based low-profile additives (LPAs), including PMMA, poly(methyl methacrylate-*co*-butyl acrylate), and poly(methyl methacrylate-*co*-butyl acrylate-*co*-maleic anhydride) with different chemical structures and MWs on the volume shrinkage characteristics and internal pigmentability for low-shrink unsaturated polyester (UP) resins during curing were investigated by an integrated approach of static phase characteristics of the ternary styrene (ST)/UP/LPA system, reaction kinetics, cured-sample morphology, microvoid formation, and property measurements. The relative volume fraction of microvoids generated during the cure was controlled by the stiffness of the UP resin used, the compatibility of the uncured ST/UP/LPA systems, and the glass-transition temperature of the LPAs used. On the basis of the Takayanagi mechanical model, the LPA mechanism on volume shrinkage control, which accounted for phase separation and microvoid formation, and factors leading to both a good volume shrinkage control and acceptable internal pigmentability for the molded parts are discussed. © 2004 Wiley Periodicals, Inc. J Appl Polym Sci 91: 3388–3397, 2004

Key words: polyesters; blends; curing of polymers; voids; structure-property relations

INTRODUCTION

The addition of specific thermoplastic polymers as low-profile additives (LPAs) in the molding compounds of unsaturated polyester (UP) resins is a well-known industrial technology. Such thermoset polymer blends, essentially made from UP, styrene (ST) monomer, and LPAs, may lead to a reduction or even the elimination of polymerization shrinkage during the cure process. A class A smooth surface for the molded part can then result.[1,2]

Among the extensive studies[3–11] on the mechanism of volume shrinkage compensation caused by LPAs, it is now generally agreed that during reaction, the LPA and crosslinked UP phases must phase separate first. Subsequent microvoid and/or microcrack formation at the interface between the LPA and the crosslinked UP phases, as well as inside the LPA phase due to microstress cracking that is initiated at the interface between the LPA and crosslinked UP phases, can then lead to volume shrinkage compensation. Other mechanisms from different standpoints have also been proposed.[1,2,8,11]

Low-profile polyester molding compounds, such as low-profile bulk-molding and sheet-molding compounds, when formulated with pigments usually exhibit an unacceptable hazing of the pigment's color. This appears to be largely the result of the refractive index (n_D) difference between the air and solid interface that occurs with microvoiding.[12,13] In general, the better the shrinkage control for the LPA is, the poorer the internal pigmentation is in terms of color depth. However, unique LPAs have now been developed[12,13] that give significantly improved deep color pigmentation with modified polyester resins and maintain a smooth surface and zero shrinkage; yet, the fundamental principle has not been treated.

In part 1 of this series of articles,[14] the chemical structure and molecular weight (MW) of poly(methyl methacrylate) (PMMA)-based LPA were demonstrated to be intimately connected with the miscibility, cure-sample morphology, curing behavior, and glass-transition temperatures (T_g's) for ST/UP/LPA systems. The objective of this study was to investigate the effects of the chemical structures and MWs of three series of PMMA-based LPAs on the volume shrinkage characteristics and internal pigmentability (L^*) for the

Correspondence to: Y.-J. Huang (yjhuang@ch.ntust.edu.tw).
Contract grant sponsor: National Science Council of the Republic of China; contract grant number: NSC 88-2216-E-011-023.

TABLE I
PMMA-Based LPAs Used in This Study

LPA code	Monomer	Molar composition[a]	M_n[b]	Polydispersity[b]	T_g (°C)[c]
PMMA1S[d]	MMA	—	22,000	3.2	106
PMMA2S[d]	MMA	—	41,000	2.9	106
MMA–BA1S	MMA, BA	0.358 : 0.642	20,000	5.1	−22.7
MMA–BA2S	MMA, BA	0.405 : 0.595	30,000	5.0	−17.5
MMA–BA–MA1S	MMA, BA, MA	0.340 : 0.611 : 0.049	41,000	1.9	−23.9
MMA–BA–MA2S	MMA, BA, MA	0.338 : 0.615 : 0.047	49,000	1.9	−23.9

[a] By ^{1}H-NMR.
[b] By gel permeation chromatography (g/mol).
[c] by DSC.
[d] 1 and 2 denote the lower and the higher molecular weights, respectively.

ST/UP/LPA systems. A mechanism resulting in both a good volume shrinkage control and acceptable L^* for the molded parts is proposed.

EXPERIMENTAL

Materials

The PMMA-based LPAs with different chemical structures and MWs were synthesized by emulsion polymerization.[14] The first series of LPAs was made from methyl methacrylate (MMA), the second series of LPAs was made from MMA and *n*-butyl acrylate (BA), and the third series of LPAs was made from MMA, BA, and maleic anhydride (MA). The six LPAs used in this study [PMMA1S, PMMA2S, MMA–BA1S, MMA–BA2S, MMA–BA–MA1S, and MMA–BA–MA2S, where MMA–BA is poly(methyl methacrylate-*co*-butyl acrylate) and MMA–BA–MA is poly(methyl methacrylate-*co*-butyl acrylate-*co*-maleic anhydride)] are summarized in Table I.

The UP resin[15] was made from MA, 1,2-propylene glycol (PG), and phthalic anhydride (PA) with a molar ratio (MR) of 0.63 : 1.01 : 0.367. The acid number and hydroxyl number were found to be 28.0 and 28.2, respectively, by end-group titration, which gave a number-average molecular weight (M_n) of 2000 g/mol. On average, the calculated number of C═C bonds in each polyester molecule was 6.79.

For the sample solution, 10 wt % LPA was added, and the MR of ST to polyester C═C bonds was fixed at MR = 2 : 1. The reaction was initiated by 1 wt % *tert*-butyl perbenzoate. For the sample solution with pigment, 10 wt % Bordeaux red, with irregular shape and nonuniform size distributions centered at 0.5–3 and 5–6 μm, was added as a red pigment.

Optical microscopy (OM)

The morphology of the sample during curing was observed with an optical microscope. One drop of sample (~0.8 mg) was placed between two microscope cover glasses; the sample was then inserted into a hot stage (Mettler, Columbus, OH, FP82HT). The cured sample at 110°C was chilled in liquid nitrogen and was subsequently observed at room temperature under an optical microscope with transmitted light at magnifications of 100–400×.

Microvoids

The quantity of microcracking in the morphology sample under OM was measured with an image analyzer.[5,9] Because the samples were of uniform thickness, the fraction of the image area that was black (because of light scattering by the microcracks) was proportional to the volume of the microcracks in the sample. Luminance values of less than 31 were taken to indicate microcracking by Mitani et al.,[5] where the scale of luminance ranged 0 (pure black) to 255 (pure white). In this work, the image of the OM photomicrograph was first input into a computer with a scanner (Epson, GT-6500, Nagano, Japan), and the lower one-fourth of the luminance scale obtained for each photomicrograph was used to calculate the relative volume fraction of microcracks and microvoids (v_m).

It should be noted that[5] the absolute quantity of microcracking could not be measured by the image analyzer system because overlapping cracks could not be distinguished, and cracks normal to the incident light do not scatter light. Another method for estimating the relative microcrack fraction include the Brunauer–Emmett–Teller (BET) surface area measurement technique demonstrated by Kinkelaar et al.,[16] but results were far from satisfactory when the microvoid size in the ST/UP/LPA cured systems was less than 0.1 μm.

Recently, in a study of carbon black filled polyethylene conductive composites, Oakey et al.[17] demonstrated that atomic force microscopy (AFM) can be used to identify void size and absolute v_m through a comparison of complementary height and phase images. In our laboratory, research is under way for the

TABLE II
Calculated Dipole Moment Per Unit Volume (μ') for the UP and LPAs, the Dipole Moment Difference Between UP and LPAs ($\mu'_{UP} - \mu'_{LPA}$), and the Isothermal Cure Conversion (α_{ISO}) for the ST/UP/LPA Systems Cured at 110°C

	μ (Debye/mol$^{1/2}$)	V (cm^3/mol)	μ' (Debye/cm$^{3/2}$)	$\mu'_{UP} - \mu'_{LPA}$	α_{ISO}[a]
UP resin					
MA–PG–PA	3.13	1,389	0.0840	—	91.8[b]
LPA					
PMMA1S	9.69	18,110	0.0720	0.0120	80.6
PMMA2S	13.22	33,710	0.0720	0.0120	69.9
MMA–BA1S	8.50	17,480	0.0643	0.0197	76.4
MMA–BA2S	10.47	26,110	0.0648	0.0192	73.5
MMA–BA–MA1S	12.41	34,840	0.0665	0.0175	71.4
MMA–BA–MA2S	13.55	41,690	0.0664	0.0176	71.6

[a] Cure conversion of total C═C bonds for the ST/UP/LPA systems as measured by DSC at 110°C.
[b] Neat UP resin at MR = 2:1.[27]

direct measurement of microvoids by AFM techniques.

Volume change

Density measurements were used to obtain volume shrinkage data. About 10 g of degassed sample solution was placed into a 10-mL density bottle, and its density at 25°C before reaction (ρ_1) was measured. The density of the sample cured isothermally at 110°C in the dilatometer (ρ_2) was also determined at 25°C by an immersion method with distilled water. The volume shrinkage was then calculated as $(1/\rho_2 - 1/\rho_1)/(1/\rho_1)$.

To monitor the volume change of the UP resins throughout the cure process, a custom-built capillary-type dilatometer was also used.[9] The volume expansion during heating from 25 to 110°C, the cure shrinkage at 110°C, and the volume contraction during cooling from 110 to 25°C was obtained. The detailed procedures were described elsewhere.[9]

Calorimetric measurements

About 2 g of degassed sample solution with 10 wt % pigment was placed in a glass mold consisting of two cover glasses (50 × 50 × 2 mm) with an o-ring (inside diameter = 22 mm and thickness = 3 mm) as the spacer. The sample solutions were cured at 110°C in a thermostated silicon oil bath for 1 h. After cooling to room temperature, the cured specimens were measured for color depth with a chromameter (Minolta, CR-300, Wanchai, Hong Kong). Ten measurements of the L^* value were taken for both sides of the specimen, respectively. For white–black pigmentation, as L^* approaches zero, the total absorption of all visible light is indicated, and the object becomes increasingly black. However, as L^* approaches 100, an increasing reflectance of visible light is indicated, and the object becomes increasingly white. Therefore, the higher the L^* value is, the lower the color depth is, and the hazing phenomenon of the cured specimen is more pronounced, leading to a worse L^*. A general rule of thumb for white–black pigmentation is that one unit of L^* value is equivalent to about a 10% tinting strength but only in the range 25–90 L^*.[13]

RESULTS AND DISCUSSION

Compatibility of the ST/UP/LPA systems

The molecular polarities of the UP resin and LPAs were evaluated in terms of the calculated dipole moment (μ) per unit molar volume (V), or $\mu/V^{1/2}$, with Debye's equation and group contribution methods in part 1 of this series of studies;[14] the results are summarized in Table II. In general, the higher the polarity difference per unit volume was between the UP and LPA, the less compatible the ST/UP/LPA system was at 25°C before the reaction. The data in Table II reveal that the sample solution containing PMMA would be theoretically the most compatible, followed by the MMA–BA–MA system and the MMA–BA system. The compatibility of the ST/UP/LPA systems during curing at 110°C, as observed from scanning electron micrographs, followed the same trend.[14] Also, for a fixed type of LPA, the addition of a higher MW LPA enhanced the degree of phase separation during curing at 110°C.

As the mixing temperature was increased from 25 to 110°C, no phase separation was observed for all six of the ST/UP/LPA ternary systems within 180 min.[14] Because the cure reaction for the ST/UP/LPA systems at 110°C ended in 60 min, all six of the systems in this study exhibited a single homogeneous phase after a phase equilibrium before the reaction at 110°C.

Cure conversion (α)

As shown in part 1 of this series of articles,[14] the addition of LPA may have led to a reduction in the

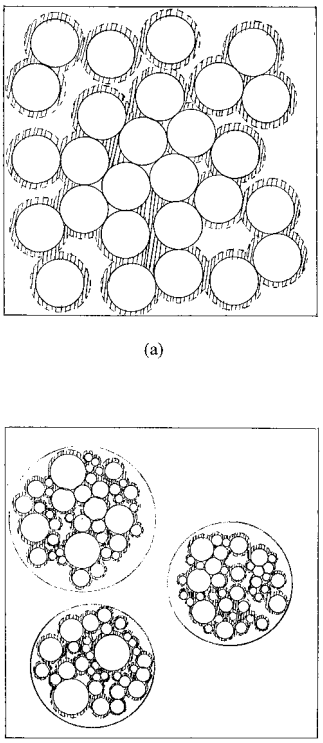

Figure 1 Schematic diagram of the fractured surface for the 10% LPA-containing sample with a MR of 2 : 1 cured isothermally at 110°C: (a) cocontinuous globule morphology and (b) two-phase microstructure. The stiff microgel particle phase is shown to be surrounded by the weak LPA-rich phase (shaded area), in which microvoids and microcracks formed during the cure.

final α for the ST/UP/LPA systems at 110°C. The most compatible PMMA1S system exhibited the highest α. Also, for a fixed type of LPA, the addition of a higher MW LPA may have generally decreased the α (Table II).

Relationship between the morphologies and mechanical properties: the Takayanagi models

Schematic diagrams for the two typical cured-sample morphologies[14] of the ST/UP/LPA systems are shown in Figure 1. Their mechanical behavior could approximately be represented by the Takayanagi models,[18–21] where arrays of weak LPA (R) and stiff ST-crosslinked polyester (P) phases are indicated (see Fig. 2) and which was described in part 1 of this series of articles[14] and can be summarized as follows.

For the systems shown in Figure 1(a), such as the PMMA1S system,[14] the microgel particles (P_1 phase) were surrounded by a layer of LPA (R phase). Between the LPA-covered microgel particles, there were some lightly ST-crosslinked polyester chains and polystyrene chains (taken both together as phase P_2), with different compositions of ST and UP from those in phase P_1, dispersed in the LPA phase (R phase). Hence, the characteristic globule microstructure could be represented by the parallel–parallel–series (P–P–S) model, as shown in Figure 2(a), which is a parallel combination of the three elements, that is, P_1, R, and P_2–R in series. In contrast, for the systems shown in Figure 1(b), such as the PMMA2S, MMA–BA, and MMA–BA–MA systems,[14] the microstructure consisted of a stiff, flake-like continuous phase of ST-crosslinked polyester (phase P_1) and a weak, globule, LPA-dispersed phase (the globule morphology could also be represented by a P–P–S model). Hence, the upper bound of mechanical behavior for the overall morphology could be represented by a parallel–parallel–parallel–series [P–(P–P–S)] model, as shown in Figure 2(b), which is simply a parallel combination of the continuous phase P_1 and the dispersed phase denoted by a P–P–S model.

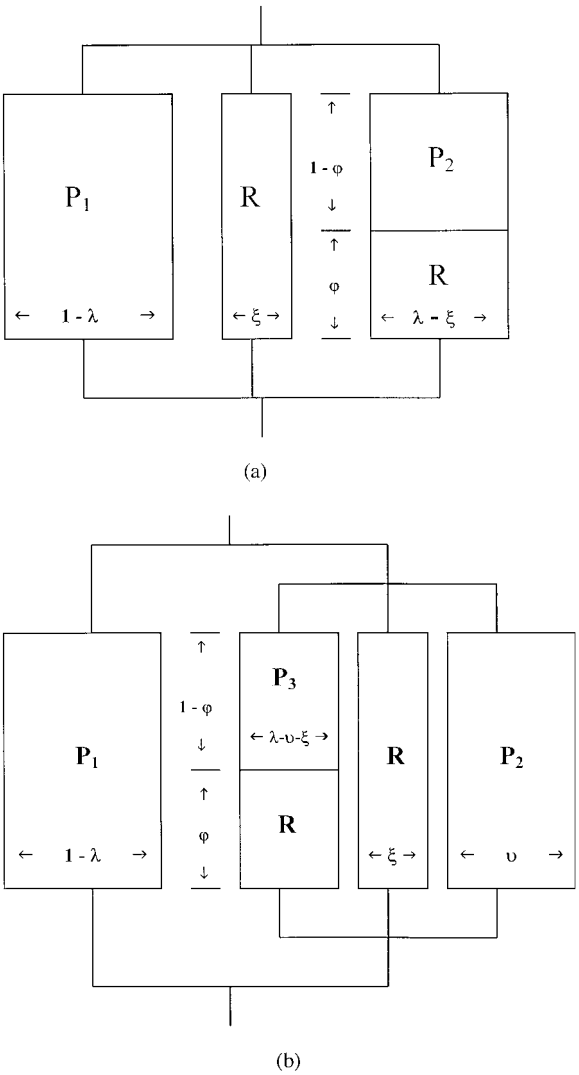

Figure 2 Takayanagi models for the mechanical behavior of cured LPA-containing UP resin systems: (a) P–P–S and (b) P–(P–P–S) models. The area of each diagram is proportional to a volume fraction of the phase.

TABLE III
Volume Shrinkage Information for the ST/UP/LPA Systems During Curing at 110°C

LPA	$\Delta V/V_0$ (%)[a]	ΔV_{tot} (%)[b]	ΔV_1 (%)[c]	ΔV_2 (%)[d]	ΔV_3 (%)[e]
Neat resin	−7.88	−8.07	3.01	−9.98	−1.10
PMMA1S	−6.20	−6.54	4.93	−10.38	−1.09
PMMA2S	−5.76	−5.89	4.25	−9.21	−0.93
MMA–BA1S	−4.93	−3.85	4.21	−7.10	−0.96
MMA–BA2S	−2.56	−2.71	3.84	−5.78	−0.77
MMA–BA–MA1S	−6.24	—	—	—	—
MMA–BA–MA2S	−6.18	—	—	—	—

[a] The estimated standard error of the measurement was 0.31%.
[b] $\Delta V_1 + \Delta V_2 + \Delta V_3$. The accuracy of the measurement was 0.01%.
[c] Volume change during heating from 25 to 110°C.
[d] Volume change during curing at 110°C.
[e] Volume change during the cooling from 110°C to 25°C.

Effects of LPAs on volume shrinkage after curing

The effects of LPAs on the fractional volume shrinkage during curing for the ST/UP/LPA systems measured by density methods are shown in Table III. The volume shrinkage of the neat UP resin was about 8%, whereas the addition of different PMMA-based LPAs reduced the volume shrinkage to about 2.5–6.5%. The effectiveness of the volume shrinkage control was ranked as MMA–BA2S > MMA–BA1S > PMMA > MMA–BA–MA. In other words, the most incompatible MMA–BA system exhibited the lowest volume shrinkage. Also, the higher the MW of LPA was, the better the volume shrinkage control was.

For the reacting systems of UP resins containing no LPA, PMMA, or MMA–BA, the three-stage volume changes due to thermal expansion of uncured resins in the heating step [ΔV_1 (25–110°C)], polymerization shrinkage during cure [ΔV_2 (110°C)], and thermal contraction of cured resin in the cooling step [ΔV_3 (110 to 25°C)] were measured by dilatometry. Figure 3 shows the fractional volume change profile for UP resins containing 10% MMA–BA2S, where a conspicuous shoulder due to microvoid formation appeared at about 60–75 min to reduce the ongoing polymerization shrinkage. This was in contrast to the neat UP system (no shoulder, not shown) and other systems (less remarkable shoulder, not shown). The variations in fractional volume changes due to the thermal expansion of the uncured resin, polymerization shrinkage, and cooling contraction of the cured resin (i.e., ΔV_1, ΔV_2, and ΔV_3) for the five systems studied are displayed in Table III, where the volume shrinkage of the finally cured sample as measured by dilatometry (ΔV_{tot}) showed very good agreement with that obtained by density measurements. As LPA was varied, the resulting change in ΔV_2 was greater than that of ΔV_1 and ΔV_3; hence, an effective LPA for volume shrinkage control would be the one that led to a significant reduction in ΔV_2 rather than favorable changes in ΔV_1 and ΔV_3.

Effects of LPA on L^* after the cure

Table IV shows the effects of LPA on L^* as the index of internal pigmentability for the ST/UP/LPA systems after the cure. Because an L^* value within 30 was recognizably dark red in tint and could be used as the acceptable upper bound for good L^* in this study, all of the systems in Table IV exhibited good L^*. On the basis of the tint in the upper side of the molded parts, the performance of L^* was ranked as neat UP resin > PMMA > MMA–BA–MA > MMA–BA. In other words, the most incompatible MMA–BA system exhibited the worst L^* (still acceptable, as mentioned previously). Also, the higher the MW of the LPA was, the worse the L^* was. Both the effects of chemical structure and MW of the LPA on L^* generally showed a reverse trend when compared with those on the volume shrinkage control.

Among the six ST/UP/LPA systems, the MMA–BA2S system provided a good volume shrinkage control [total volume change as measured by density

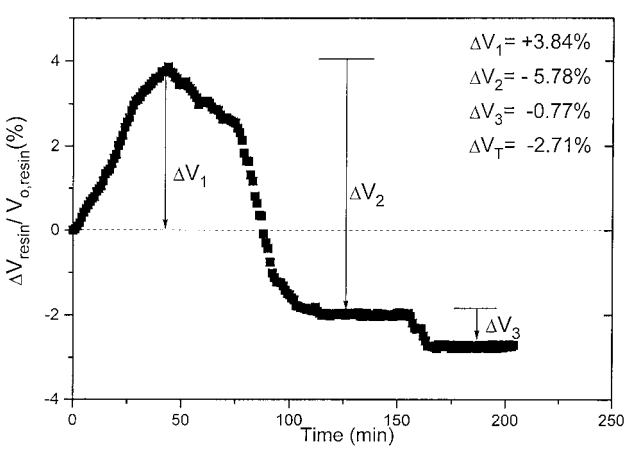

Figure 3 Fractional volume change profiles for the low-shrink UP resin at a MR of 2 : 1 containing 10 wt % MMA–BA2S as an LPA under three stages of heating (25–110°C), curing at 110°C, and cooling (110 to 25°C). $\Delta V_T = \Delta V_1 + \Delta V_2 + \Delta V_3$.

TABLE IV
L^* Values as the Index of Internal Pigmentability for Both Sides of the Molded Parts for the ST/UP/LPA Systems After Isothermal Curing at 110°C

LPA	L^* (upper side)	L^* (bottom side)
Neat resin	22.24 (0.03)	23.08 (0.06)
PMMA1S	24.96 (0.05)	25.89 (0.03)
PMMA2S	25.25 (0.06)	26.12 (0.06)
MMA–BA1S	27.82 (0.09)	26.62 (0.05)
MMA–BA2S	28.84 (0.08)	28.12 (0.07)
MMA–BA–MA1S	24.63 (0.03)	28.80 (0.05)
MMA–BA–MA2S	26.24 (0.05)	27.69 (0.02)

The values in parentheses are the estimated standard errors for a sample mean of 10 measurements.

methods ($\Delta V/V_0$) $\cong -2.6\%$] and achieved an acceptable L^* ($\cong$ 29).

Effects of microvoid formation on volume shrinkage control

Pattison et al.[3,4] proposed that as the crosslinking of LPA-containing UP resins proceeds, strain due to polymerization shrinkage develops in the system, particularly at the interface of the LPA phase and crosslinked UP phase. This strain can increase to the point that stress cracking propagates through the weak LPA phase, relieving this strain, forming microcracks and/or microvoids, and compensating for the overall volume shrinkage by the microcrack or microvoid space.

Table V shows the relative v_m values for the varied ST/UP/LPA systems. The relative v_m was the highest for the most incompatible MMA–BA system, followed by the PMMA and MMA–BA–MA systems. Also, the higher the MW of the LPA was, the higher the relative v_m was. A comparison with experimental results in Tables III and V indicated that greater microvoid formation may have given less volume shrinkage, which generally supports the volume shrinkage mechanism of strain relief through stress cracking.

In Table V, relative v_m values as high as 25–35% for the MMA–BA systems were due to the image analysis on OM photomicrographs, which did not allow direct measurement for the absolute v_m, as mentioned earlier. Nevertheless, the relative v_m among the systems could be reasonably compared by this method.

It should be pointed out that the overall volume change after curing could not be solely determined by the volume compensation for shrinkage due to a microvoid formation. The intrinsic polymerization shrinkage of the resin system was also important in the determination of the overall volume change.[9] In general, in the cure of UP at 110°C, a higher ST content may have enhanced the intrinsic polymerization shrinkage (i.e., ΔV_2 in Fig. 3 corrected for any possible volume compensation by microvoids and microcracks), especially when the MR of ST to polyester C═C bonds was greater than 2 : 1, where the final conversion at 110°C greatly increased with ST content.[22]

Effects of microvoid formation on L^*

Atkins and Rex[12] pointed out that the microvoid formation is also intimately connected with the L^* of molded parts. As incident light entered an internally pigmented part of the cured ST/UP/LPA system, the intensity of reflective light to the pigment is greatly reduced because of the severe light scattering that occurs at the solid/air (microvoid) and UP/LPA interfaces inside the parts, leading to the hazing of a pigment's color. Because the difference in n_D between the solid/air interface of a microvoid and that of UP/LPA is approximately 0.5 and 0.05, respectively (the n_D's for air, UP, and PMMA are 1.00, 1.54, and 1.49, respectively, as reported by Atkins and Rex), the dominant factor in the hazing of a pigment's color is the presence of microvoids.

In this study, on the basis of Lorentz and Lorenz formula,[23] the n_D's for the MA–PA–PG type of UP, PMMA, MMA–BA, and MMA–BA–MA were calculated to be 1.587, 1.516, 1.509, and 1.394, respectively (for polystyrene, n_D = 1.603), and the difference in the n_D values between UP and the PMMA-based LPA ranged from 0.07 to 0.19. Indeed, it was the difference in the n_D values of UP and LPA with air (n_D = 1.000), which ranged from 0.39 to 0.59, that actually mattered for the L^* of the ST/UP/LPA cured system. That was the reason why the higher the v_m was (MMA–BA > PMMA > MMA–BA–MA), the worse the L^* was in terms of more pigment hazing, as revealed by a higher L^* value on the upper side of the molded parts (compare Tables IV and V).

TABLE V
Relative v_m for Samples of the ST/UP/LPA Systems After Isothermal Curing at 110°C

LPA	Relative v_m (%)
Neat resin	0[a]
PMMA1S	5.10
PMMA2S	6.71
MMA-BA1S	25.47
MMA-BA2S	35.20
MMA-BA-MA1S	5.32
MMA-BA-MA2S	5.87

[a] For the cured neat UP resin system, the relative v_m was taken as zero because the scale of luminance was greater than 150, which was much greater than the lower one-fourth of the luminance scale for all of the ST/UP/LPA cured systems.

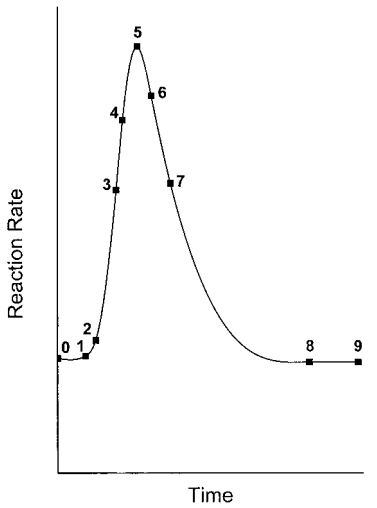

Figure 4 Schematic DSC reaction rate profile of the ST/UP/LPA systems at 110°C. The eight steps involved in the LPA action during the cure are designated.

Effect of the LPA mechanism on volume shrinkage control

For the ST/UP/LPA systems with two-phase microstructures, such as PMMA2S, MMA–BA, and MMA–BA–MA, a P–(P–P–S) mechanical model was proposed, as mentioned earlier. In light of the detailed morphological changes[24] during the entire cure reaction for a typical ST/UP/PMMA system with a two-phase morphology and the results in part 1 of this series of articles,[14] the LPA mechanism on volume shrinkage control, with the aid of the Takayanagi mechanical model shown in Figure 2(b), is proposed as follows. Eight steps were involved in the LPA action during the entire cure reaction at 110°C, and the corresponding schematic differential scanning calorimetry (DSC) reaction rate profile, with the eight steps designated along the curve, is shown in Figure 4 to facilitate the in-depth analysis:

1. Heating step: This step corresponds to the interval [0,1] in Figure 4. For the ST/UP/LPA system with a phase separation at 25°C in this study, on heating from 25°C to the cure temperature 110°C, it appeared as a single homogeneous phase before the reaction, and no global phase separation was observed.[14] At this step, the system volume increased because of the thermal expansion (ΔV_1 as shown in Fig. 3). If the system without reaction was not miscible at 110°C, phase separation, on a microscopic level, occurred during heating. Thus, the time for heating before the reaction exotherm was observed had an influence on the final morphologies, which, in turn, affected the volume shrinkage control.
2. Incipient phase-separation step: This step corresponds to the interval [1,2] in Figure 4. As the crosslinking reaction proceeded isothermally at 110°C, reaction-induced phase separation into a continuous phase [P_1 phase in Fig. 2(b)], which was UP and ST rich, and an LPA-dispersed phase [P_2, P_3, and R phases in Fig. 2(b)], which was ST and LPA rich, occurred at a very low α ($\alpha < 1\%$),[24] where the whole system was fluid like. Some primary microgel particles (P_2 phase) were observed in the LPA-dispersed phase. At this step, the system volume decreased somewhat because of the polymerization shrinkage (small part of ΔV_2, as shown in Fig. 3). The onset of phase separation during the cure depended on the ST/UP/LPA ternary behavior of the systems, as could be controlled by the chemistry and MW (distribution) of the UP and LPA.
3. Gelation step: This step corresponds to the interval [2,3] in Figure 4. As the α increased, the mass transfer into or out of the continuous and LPA-dispersed phases proceeded, and a drift of compositions for ST, UP, and LPA in either phase then persisted. Meanwhile, more and more microgel particles [P_2 phase in Fig. 2(b)] formed but tended to be fused together in the LPA-dispersed phase, which was in contrast to a lack of microgel particle precipitation in the continuous phase (P_1 phase) due to the inadequate segregating effect of LPA (R phase) on the microgel particles formed therein. Near the gelation point ($\alpha \approx 10$–15%),[25] corresponding to point 3 in Figure 4, the translational diffusion for the large molecules, such as UP and LPA, essentially ceased because viscosity tended to infinity. However, the diffusion of ST, which is a small molecule, and the segmental diffusion of the UP and LPA still proceeded in the lightly crosslinked, ST swollen network. Nevertheless, because the long-range diffusion of ST that crossed phase boundaries was considerably curtailed, the compositions in the continuous and LPA-dispersed phases remained virtually unchanged near the gelation. When compared with the incipient phase-separation stage, the microgel particles in the LPA-dispersed phase became more independent and clearly identified because of the ever-increasing phase separation, whereas the continuous phase appeared more gel-like because of further crosslinking. At this step, the system volume continued to decrease because of further polymerization shrinkage, but the net change of the system volume was still positive.[9] [Gelation occurred at about 50 min, as referred to in the curve shown in Fig. 3, where the times at the end of the heating stage from 25 to 110°C (i.e., maximum point of the curve), for microvoid formation, at a zero system volume change and at the end of

cure were 43, 60–75, 80, and 110 min, respectively.)

4. Gel to rubbery solid transition step: This step corresponds to the interval [3,5] in Figure 4. As the crosslinking reaction further progressed ($\alpha \approx 25$–35%, where the DSC rate profile exhibited the gel effect,[14] and approached the maximum point in Fig. 4), the gel state transformed to the rubbery solid for all of the phases, the rate of which depended on the cure reaction rate in each phase.
5. Residual strain generation step: This step corresponds to the interval [5,6] in Figure 4. As the crosslinking reaction proceeded, the flake-like microstructure of the major continuous ST-crosslinked polyester phase [P_1 phase in Fig. 2(b)], as well as the microgel particle phase [P_2 phase in Fig. 2(b)], together with the LPA-rich phase [i.e., phases R and P_3 as a whole in Fig. 2(b)], became so compact that residual strain due to polymerization shrinkage developed in the system, particularly at the interface of the LPA-rich phase and densely crosslinked UP phase (P_1 and P_2 phases). In general, the higher the Young's modulus of the densely crosslinked polyester phases (P_1 and P_2 phases) was, the lower the polymerization strain of those densely crosslinked polyester phases (ε_{Pi}) was, which led to a lower residual strain at the interface.
6. Major microvoid and microcrack formation step: This step corresponds to the interval [6,7] in Figure 4. As the crosslinking reaction continued and the reaction rate remained high, the residual strain at the interface increased to the point [i.e., the yield strain of the LPA-rich phase (ε_{YR})] that stress cracking propagated through the weak LPA-rich phase. This greatly relieved the strain, forming microcracks and/or microvoids caused by local premature failure of the weak rubbery phase and compensating for the overall volume shrinkage by the microcrack or microvoid space. It was around 50% monomer conversion (the interval [6,7] in Fig. 4), where the DSC rate profile descended shortly after the maximum point, that microvoids and microcracks developed markedly in the system.[9,24] Furthermore, at such an extent of α, all of the phases were in the rubbery solid state, with the crosslinking density for the LPA-rich phase lower than that of the other phases, which greatly facilitated the formation of microvoids and microcracks in the LPA-rich phase. This was because vitrification was too far away to result in a rigid phase with a high Young's modulus and to prevent premature local failure (i.e., microvoid formation) for the weak LPA-rich phase.
7. Minor microvoid and microcrack formation step: This step corresponds to the interval [7,8] in Figure 4. As the reaction conversion increased ($\alpha \approx 60$–65%, shown as point 7 in Fig. 4) until the final conversion ($\alpha \approx 70$–80%, shown as point 8 in Fig. 4), the polymerization shrinkage persisted in each phase (ΔV_2 as shown in Fig. 3). Meanwhile, the rate of microvoid and microcrack formation was greatly reduced because of both the decrease in ε_{Pi} caused by the decreasing polymerization shrinkage force as a result of a reduction in the reaction rate (see the later stage of the reaction rate profile in Fig. 4), which decreased the extent of stress cracking, and the increase in ε_{YR} caused by the increasing crosslinking density therein and the concomitant approaching of vitrification, which resisted the microvoid formation.
8. Cooling step: This step corresponds to the interval [8,9] in Figure 4. On cooling from 110°C to the room temperature (25°C), the system volume decreased because of thermal contraction (ΔV_3 as shown in Fig. 3). Meanwhile, microvoids inside the molded part propagated throughout the weak LPA-rich phase, thereby relieving the molded part of thermal stresses. This was the reason why an internally pigmented part of the ST/UP/LPA system was deeply colored when first removed from a hot mold but became increasingly hazed in its color. At this step, the increase of microvoid volume caused by the relief of thermal stress did not make up for the decrease in volume due to the cooling contraction, which led to a negative value of ΔV_3, as shown in Table III.

Factors affecting both good volume shrinkage control and acceptable L^*

For the MA–BA2S system, the relatively high v_m ($\approx$ 35%) could have led to better volume shrinkage control yet worse L^*. However, the latter was not observed. This may have resulted from the fact that its two-phase microstructure [Fig. 1(b)], consisting of a microvoid-free flake-like continuous phase and a microvoid-rich globule LPA-dispersed phase, provided a pathway for the reflective light to the pigment to pass through the sample via the microvoid-free flake-like continuous phase even though the reflective light may have possibly experienced multiple scattering within the LPA-dispersed phase. Consequently, the hazing of the pigment's color was prevented.

However, if the reflective light to the pigment were to have experienced infinite amount of light scattering within the LPA-dispersed phase, the hazing of a pigment's color may have still resulted. Hence, we inferred that either the v_m or the average size of the

microvoids (s_m) were small enough to achieve an acceptable L^*. In theory, as s_m increased larger than 0.02–0.04 μm, which was about 1/20 of the wavelength of visible light (the wavelength of visible light ranges from 0.45 to 0.75 μm.), the light scattering caused by such a size of microvoids may have become increasingly significant. In our previous work,[24] an s_m about 1 μm in diameter within the LPA-dispersed phase and a microcrack 1–2 μm wide along the interface between the LPA-rich phase [i.e., phases R and P_3 as a whole in Fig. 2(b)] and the major continuous crosslinked UP phase [i.e., phase P_1 in Fig. 2(b)] were observed. Therefore, either s_m was smaller or v_m was lower; the light scattering within the sample could only possibly behave in such a way that the scattered light that would otherwise travel permanently within the LPA-dispersed phase would eventually pass through the sample via the microvoid-free flake-like continuous phase, leading to minimum hazing of the pigment's color.

For the MMA–BA2S system with a relatively high v_m, the s_m in the LPA-dispersed phase was small enough to meet the requirement for acceptable L^*.

Effects of the stiffness of the UP resin, the degree of phase separation, the cured-sample morphology, and the T_g of LPA on microvoid formation

Microvoids and microcracks essentially exist in the phase region with a cocontinuous globule microstructure, where the interface generated between the LPA-rich phase and the densely crosslinked UP phase makes possible strain relief through stress cracking and the subsequent formation of microvoids and microcracks in the weak LPA-rich phase (i.e., shaded area in Fig. 1). Therefore, v_m depended on three factors, namely, ε_{Pi} [in phase P_1 in Fig. 2(a) and phases P_1 and P_2 in Fig. 2(b)], the interfacial area between LPA-rich phase and the densely crosslinked UP phase (A_i), and ε_{YR}. In contrast, s_m depended on two factors, namely, ε_{Pi} and ε_{YR}.

As mentioned earlier, all of the phases were in the rubbery state instead of the glassy state at about 50% of monomer conversion, where microvoids and microcracks could develop significantly in the system. ε_{Pi} could be controlled by the Young's modulus in the rubbery region for the densely crosslinked polyester phases, which may have depended on the chain stiffness of the UP resin used and the MR of ST consumed to polyester C═C bonds reacted in the densely crosslinked polyester phases as a result of reaction-induced phase separation during the cure. A_i could be controlled by the cured-sample morphology and the degree of phase separation during the cure, and in turn, the compatibility of the uncured ST/UP/LPA system. ε_{YR} could be controlled by the temperature difference between the T_g of the LPA used and the cure temperature (ΔT), the LPA concentration and the MR in the LPA-rich phase as a result of reaction-induced phase separation during the cure. ΔT was equivalent to the effect of vitrification, which could markedly influence the Young's modulus and the expansion coefficient for the LPA-rich phase. As vitrification approaches either for the major or the minor step of microvoid formation in the LPA-rich phase (i.e., intervals [6,7] and [7,8], respectively, in Fig. 4), this could lead to less microvoid formation therein. That was why the most polymerization shrinkage was observed near the end of the reaction exotherm with very little and ever-decreasing microvoid formation (i.e., later part of ΔV_2 in Fig. 3), which fell in the region where vitrification was probably starting.

A lower stiffness of UP resin, a somewhat incompatibility of the uncured ST/UP/LPA system that could lead to the generation of sufficient A_i during the cure, and a lower T_g of the LPA in reference to the cure temperature (i.e., a higher ΔT) could result in a higher v_m during the cure. However, either the lower ε_{Pi} in the densely crosslinked polyester phases or the lower ε_{YR} in the LPA-rich phase could lead to a smaller s_m. The effects of cured-sample morphology, degree of reaction-induced phase separation, stiffness of the UP resin, T_g of LPA, and cure temperature on v_m and s_m and their associated reasoning were summarized in our recent publication.[26]

In this study, A_i was greater for the PMMA1S system (with a cocontinuous globule microstructure) than for the MMA–BA and the MMA–BA–MA systems (with a two-phase microstructure). However, PMMA was only 4°C above its T_g (106°C) at the cure condition of 110°C, which was in contrast to the 127–134°C above their T_g's for MMA–BA (−17 to −23°C) and MMA–BA–MA (−24°C; i.e., ΔT was much smaller for the former case). Hence, the much higher v_m for the least compatible MMA–BA systems than for the most compatible PMMA1S system (25–35 vs. 5%) was due to the favorable effect of the lower T_g for the LPA predominating over the adverse effect of a smaller A_i on the microvoid formation for the former systems. As for the MMA–BA–MA system, although it was more compatible than the MMA–BA system, a two-phase microstructure with a greater reduction in the number of LPA-dispersed phase resulted,[14] which could greatly reduce A_i and, in turn, v_m (5–6% vs. 25–35%). For a fixed type of LPA, increasing LPA MW enhanced phase separation during the cure, and A_i increased, leading to a higher v_m (Table V).

CONCLUSIONS

The effects of PMMA-based LPAs with different chemical structures and MWs on volume shrinkage characteristics and L^* for ST/UP/LPA systems were investigated with an integrated approach of static

phase characteristics, cured-sample morphology, reaction kinetics, microvoid formation, and property measurements. On the basis of the Takayanagi mechanical model, factors leading to both a good volume shrinkage control and acceptable L^* for the molded parts were proposed.

At around 50% monomer conversion with a high reaction rate caused by the gel effect, where the sample transformed to a rubbery solid state and the residual polymerization strain at the interface exceeded ε_{YR}, that microvoids and microcracks could develop markedly in the system. The microvoid formation during the cure of the ST/UP/LPA system was closely connected not only with the volume shrinkage control but also with the L^*. In general, a higher v_m led to a better volume shrinkage control but to more hazing of a pigment's color.

For the ST/UP/LPA system, both by designing a two-phase microstructure for the cured sample that contained a microvoid-free flake-like continuous phase and a globule LPA-dispersed phase with sufficient microvoids and microcracks therein and by controlling the s_m small enough to reduce light scattering at the solid/air (microvoid) interface, we achieved both a good volume shrinkage control and an acceptable L^*.

The v_m depended on ε_{Pi}, A_i, and ε_{YR}. The first factor could be controlled by the stiffness of UP resin used; the second factor could be controlled by the cured-sample morphology and, in turn, the compatibility of the uncured ST/UP/LPA system; and the third factor was influenced by ΔT or the vitrification in the LPA-rich phase.

s_m of the microvoids generated during the cure generally depended on both ε_{Pi} and ε_{YR}.

In this study, the use of an MA–PG–PA type of UP resin (MR of MA and PA $\cong$ 0.63 : 0.37) and an MMA–BA2S type of LPA (M_n = 30,000 g/mol, T_g = −24°C, and MR of MMA and BA $\cong$ 0.40 : 0.60) under an isothermal cure at 110°C achieved a good volume shrinkage ($\Delta V/V_0$ = −2.6%) and an acceptable L^* (L^* = 29).

References

1. Bartkus, E. J.; Kroekel, C. H. Appl Polym Symp 1970, 15, 113.
2. Atkins, K. E. In Sheet Molding Compounds: Science and Technology; Kia, H. G., Ed.; Hanser: New York, 1993; Chapter 4.
3. Pattison, V. A.; Hindersinn, R. R.; Schwartz, W. T. J Appl Polym Sci 1974, 18, 2763.
4. Pattison, V. A.; Hindersinn, R. R.; Schwartz, W. T. J Appl Polym Sci 1975, 19, 3045.
5. Mitani, T.; Shiraishi, H.; Honda, K.; Owen, G. E. In Proceedings of the 44th Annual Conference, Cincinnati, OH; SPI Composites Institute: New York, 1989; p 12F.
6. Suspene, L.; Fourquier, D.; Yang, Y. S. Polymer 1991, 32, 1593.
7. Hsu, C. P.; Kinkelaar, M.; Hu, P.; Lee, L. J. Polym Eng Sci 1991, 31, 1450.
8. Bucknall, C. B.; Partridge, I. K.; Phillips, M. J. Polymer 1991, 32, 636.
9. Huang, Y. J.; Liang, C. M. Polymer 1996, 37, 401.
10. Li, W.; Lee, L. J. Polymer 2000, 41, 697.
11. Zhang, Z.; Zhu, S. Polymer 2000, 41, 3861.
12. Atkins, K. E.; Rex, G. C. Proceedings of the 48th Annual Conference, Cincinnati, OH; SPI Composites Institute: New York, 1993; p 6D.
13. Atkins, K. E.; Rex, G. C.; Reid, C. G.; Seats, R. L.; Candy, R. C. Proceedings of the 47th Annual Conference, Cincinnati, OH, SPI Composites Institute: New York, 1992; p 7D.
14. Dong, J.-P.; Huang, J.-G.; Lee, F.-H.; Roan, J.-W.; and Huang, Y.-J. J Appl Polym Sci 2004, 91, 3369.
15. Huang, Y. J.; Jiang, W. C. Polymer 1998, 39, 6631.
16. Kinkelaar, M.; Wang, B.; Lee, L. J. Polymer 1994, 35, 3011.
17. Oakey, J.; Marr, D. W. M.; Schwartz, K. B.; Wartenberg, M. Macromolecules 2000, 33, 5198.
18. Huang, Y. J.; Chen, L. D. Polymer 1998, 39, 7049.
19. Takayanagi, M.; Imada, K.; Kajiyama, T. J Polym Sci Part C 1966, 15, 263.
20. Ward, I. M.; Hadley, D. W. An Introduction to the Mechanical Properties of Solid Polymers; Wiley: New York, 1993; p 154.
21. Sperling, L. H. Introduction to Physical Polymer Science, 3rd ed.; Wiley: New York, 2001; Chapter 10, p 438.
22. Huang, Y. J.; Su, C. C. J Appl Polym Sci 1995, 55, 305.
23. Van Krevelen, D. W. Properties of Polymers, 3rd. ed.; Elsevier: London, 1990; pp 198, 292.
24. Huang, Y. J.; Su, C. C. J Appl Polym Sci 1995, 55, 323.
25. Huang, Y. J.; Su, C. C. Polymer 1994, 35, 2397.
26. Huang, Y. J.; Chen, T. S.; Huang, J. G.; Lee, F. H. J Appl Polym Sci 2003, 89, 3336.
27. Lee, S. C. M.S. Thesis, National Taiwan University of Science and Technology, 1998.